INSTITUTE OF PHYSICS PUBLISHING SUPERCONDUCTOR SCIENCE AND TECHNOLOGY

Supercond. Sci. Technol. **16** (2003) 809–814 PII: S0953-2048(03)61076-6

Time evolution and spatial distribution of temperature in YBCO bulk superconductor after pulse field magnetizing

Hiroyuki Fujishiro[1], Tetsuo Oka[2], Kazuya Yokoyama[2] and Koshichi Noto[1]

[1] Faculty of Engineering, Iwate University, 4-3-5 Ueda, Morioka 020-8551, Japan
[2] Iwate Industrial Promotion Center, 3-52-2, Iioka-shinden, Morioka 020-0852, Japan

E-mail: fujishiro@iwate-u.ac.jp

Received 13 March 2003, in final form 14 May 2003
Published 11 June 2003
Online at stacks.iop.org/SUST/16/809

Abstract
The time evolutions of temperature rise $\Delta T(t)$ after pulse field magnetizing have been measured on the surface of a cryo-cooled YBaCuO bulk superconductor. The temperature rise ΔT increases with increasing pulse field strength, and a quite large temperature rise ($\Delta T_{max} \sim 18.8$ K) is observed just before the trapped magnetic flux reaches the central region of the bulk. The epoxy resin, impregnated and coated to the bulk crystal for mechanical reinforcement, prevents the heat exhaust towards the cold stage of the refrigerator and it needs much time to recover its initial temperature. The spatial distribution of $\Delta T(t)$ has indicated that the magnetic fluxes tend to enter into the bulk, avoiding the 4-fold growth sector boundaries of the bulk crystal.

1. Introduction

For the application of bulk superconductors as a high strength magnet, the pulse field magnetizing (PFM) method is a useful technique as well as the static field cooled magnetizing (FCM) method [1]. Recently, a new PFM method based on a series of iterative magnetizing operations with gradually reduced pulse field amplitudes, named the IMRA method, has been proposed [2]. In this method, the PFM operations are repeated so as to efficiently enhance the total trapped magnetic fluxes in the bulk. It was demonstrated that, by the IMRA method, the YBaCuO bulk could trap almost an equal amount of the magnetic flux as the FCM method in liquid nitrogen [3]. However, at temperatures lower than 77 K, the maximum trapped magnetic flux by PFM even using the IMRA method is generally lower than that by FCM as shown for the SmBaCuO bulk superconductors [4, 5]. A possible origin for this observation can be the temperature rise caused by the viscous motion of the magnetic fluxes, resulting in the decrease of the trapped field. The realization of the trapped magnetic field by PFM below 77 K as high as that of FCM is greatly desired because the use of a cryo-cooled refrigerator is now very popular to cool the bulk superconductors far below 77 K.

Ikuta *et al* measured the *in situ* local magnetic flux density of YBaCuO and SmBaCuO bulks in liquid nitrogen just after PFM, and then calculated the time and position dependences of the temperature rise ΔT at the bulk surface [6]. The estimated ΔT initially increases rapidly and reaches a maximum within the order of a millisecond. The temperature rises faster in the outer side of the bulk. The estimated ΔT is only a few K and increases with increasing pulse field strength. These calculations, however, have not been testified by experiments. There have been no calculations nor experimental data as for the time and position dependences of the temperature rise $\Delta T(t, r)$ of the bulk superconductors cooled by a cryo-cooled refrigerator. Recently, the epoxy resin impregnation technique for the bulk materials has been widely applied for the mechanical reinforcement [7]. The existence of the low-thermal-conductive epoxy resin on the bulk surface may prevent the heat exhaust from the bulk and enhance the temperature rise after PFM. However, there have been no

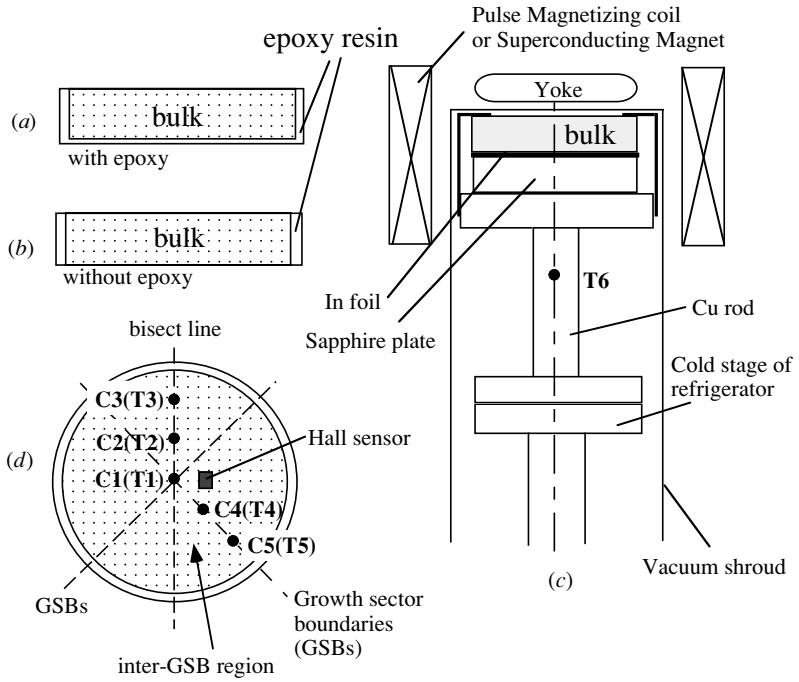

Figure 1. The experimental setup of the YBaCuO bulk superconductor for the temperature measurements. The cross sections of the bulk for (*a*) 'with epoxy' and (*b*) 'without epoxy' settings are shown. (*c*) The setting of the bulk in the Gifford McMahon (GM) cycle helium refrigerator and the position of the temperature measurement $T6$ are shown. (*d*) The positions of the temperature measurement $T1$–$T5$ on the bulk surface are indicated (see the text).

experimental data for the effect of the resin-impregnation on ΔT of the bulks either.

In this paper, we report and analyse the time and position dependences of the temperature rise $\Delta T(t, r)$ after PFM for the YBaCuO bulk superconductors with and without epoxy resin, which are cooled using a cryo-cooled refrigerator down to ∼40 K.

2. Experimental details

Figure 1 shows the setup of the YBaCuO bulk superconductor in a Gifford McMahon (GM) cycle helium refrigerator (AISIN, GR103). The YBaCuO bulk superconductor used in this study is a highly *c*-axis-oriented crystal fabricated by Dowa Mining Co, Ltd. The crystal consists of $YBa_2Cu_3O_y$ (Y123), Y_2BaCuO_5 (Y211) with the molar ratio of 1.0 : 0.4 and 0.5 wt% Pt powder (without Ag_2O addition). The initial size of the bulk is 46 mm in diameter and 15 mm in thickness. The bulk was uniformly impregnated and coated by epoxy resin in vacuum, the final sample size being 52 mm in diameter and 17 mm in thickness. The epoxy resin layer (∼1 mm in thickness) on the upper side of the bulk was removed in order to measure the precise temperature of the bulk surface as shown in figure 1(*a*). We name this sample setting as the 'with epoxy' setting. In the setting shown in figure 1(*b*), the epoxy resin on the lower side was also removed, which we name as the 'without epoxy' setting.

The YBaCuO bulk was stuck on the sapphire plate on the cold plate of the GM refrigerator using an indium (In) foil as shown in figure 1(*c*). Five sets of Teflon-coated chromel–constantan thermocouples (76 μm in diameter) were adhered to the bulk surface using GE7031 varnish (figure 1(*d*)). The thermocouple at the centre of the bulk is named as C1 and three thermocouples (C1, C4, C5) were aligned along one of the 4-fold growth sector boundaries (GSBs) with a 9 mm distance. GSBs are a kind of grain boundaries which are formed in the *ab*-plane of the bulk sample as a result of the collision of the crystal growth fronts [1]. The other two thermocouples (C2, C3) were set along a line which makes an angle of 135° from the first GSB line with a same distance. We name this line, along which the thermocouples (C1, C2, C3) were put, as the bisect line, and the sector region surrounded by GSBs, as the inter-GSB region. We denote the temperatures measured by C1–C5 as $T1$–$T5$. The temperature of the cold stage of the GM refrigerator, $T6$, was also monitored. Since the magnetic field dependence of the thermoelectric voltage of the chromel–constantan thermocouple used in this experiment is within 2% under the field of 5 T and at 40 K [8], the recalibration of the thermoelectric voltage in the field was not performed. Each thermocouple voltage was monitored about seven times per second just after applying the pulse fields. The cryo-cooled YBaCuO bulk was magnetized using a pulse coil dipped in liquid N_2 as shown in figure 1(*c*). The rise time of the pulse was about 1 ms. The strength of the pulse field B_{ex} was calculated from the current flowing through the coil. B_{ex} was applied iteratively following a typical IMRA procedure. The Hall sensor (F W Bell, model BHA 921) was adhered to the position with a 3 mm distance from the bulk centre as shown in figure 1(*d*), which monitored the trapped magnetic field ${B_T}^P$. The trapped field ${B_T}^{FC}$ following FCM using the cryo-cooled superconducting magnet was also measured at several temperatures. In the FCM procedure, the static magnetic field of 5 T was decreased down to 0 T in 18 min (0.278 T min^{-1}). The distribution of the trapped magnetic flux density was mapped using an axial-type Hall censor, which was scanned 3 mm above the bulk surface.

Table 1. Summary of the IMRA method for each applied pulse in the case of the 'without epoxy' setting; the applied pulse field B_{ex}(T), the maximum temperature rise $\Delta T\,1_{max}$(K) at the centre of the bulk, the maximum temperature of $T\,1_{max}$(K) and the trapped field measured by the attached Hall sensor $B_T{}^P$(T).

Pulse	B_{ex} (T)	$\Delta T\,1_{max}$ (K)	$T\,1_{max}$ (K)	$B_T{}^P$(T)
# 1	2.322	3.7	46.0	0.056
# 2	3.014	4.3	45.5	0.013
# 3	3.870	18.8	59.8	0.271
# 4	4.644	19.2	60.0	2.029
# 5	5.418	24.5	66.0	2.278
# 6	5.031	21.7	63.0	2.350
# 7	4.644	18.5	60.0	2.394
# 8	2.418	14.0	56.0	2.418
# 9	3.870	9.8	52.5	2.403
#10	3.014	4.5	47.5	2.437
#11	2.322	1.7	44.7	2.438

3. Results and discussion

3.1. Temperature rise under pulse field magnetizing

The GM refrigerator used in this study needs about 3 h to cool the cold stage with the YBaCuO bulk superconductor to the lowest temperature ($T = 35$ K). However, the time to reach the lowest temperature at the bulk sample surface are very different between the 'with epoxy' and 'without epoxy' settings; the former takes about 9 h, while the latter takes about 3.5 h. One of the authors (HF) and co-workers measured the anisotropy of the thermal conductivity $\kappa(T)$ and the thermal diffusivity $\alpha(T)$ of the YBaCuO bulk superconductors prepared in the same procedure [9]. The $\kappa(T)$ values in the ab-plane (κ_{ab}) and along the c-axis (κ_c) are $\kappa_{ab} = 98$ and $\kappa_c = 23$ mW cm^{-1} K^{-1} at 200 K, and $\kappa_{ab} = 185$ and $\kappa_c = 30$ mW cm^{-1} K^{-1} at 40 K, respectively. In comparison to those κ values, $\kappa(T)$ of the used epoxy resin is quite low (1.8 mW cm^{-1} K^{-1} at 293 K) [7]. The difference of the reaching time to the lowest temperature between the 'with epoxy' and 'without epoxy' settings may come from the existence of low-thermal-conductive epoxy resin with 1 mm in thickness between the cold stage and the YBaCuO bulk. The lowest temperatures of the bulk surface, $T\,1$–$T\,5$ were about ∼42 K for both settings and about 7 K higher than $T\,6$. The vacuum gap between the bulk surface and the inner surface of the vacuum shroud is only 1.5 mm and the radiation heat should intrude into the bulk, which may be the main origin of the temperature rise at the bulk surface. The temperature rise of 7 K results from the low thermal conductivity and the large thickness along c-axis of the bulk superconductor. Although a sufficient vacuum gap may reduce the temperature difference, the high trapped magnetic field cannot be fully utilized at the outer surface of the vacuum shroud because of the elongated distance from the bulk surface.

Table 1 numerically summarizes the strength of the pulse field B_{ex}, the maximum temperature rise $\Delta T\,1_{max}$ of $T\,1$, the maximum temperature $T\,1_{max}$ and the trapped field $B_T{}^P$ measured by the attached Hall sensor after each B_{ex} application. In the 'without epoxy' setting, 11 magnetic pulses, which we abbreviate to #1 to #11 in order, were applied after the bulk surface temperature $T\,1$ recovers to the initial temperature (∼42 K). In the 'with epoxy' setting, the same series of the 11 magnetic pulses B_{ex} were applied with every 20–30 min time interval before $T\,1$ recovers to the initial temperature.

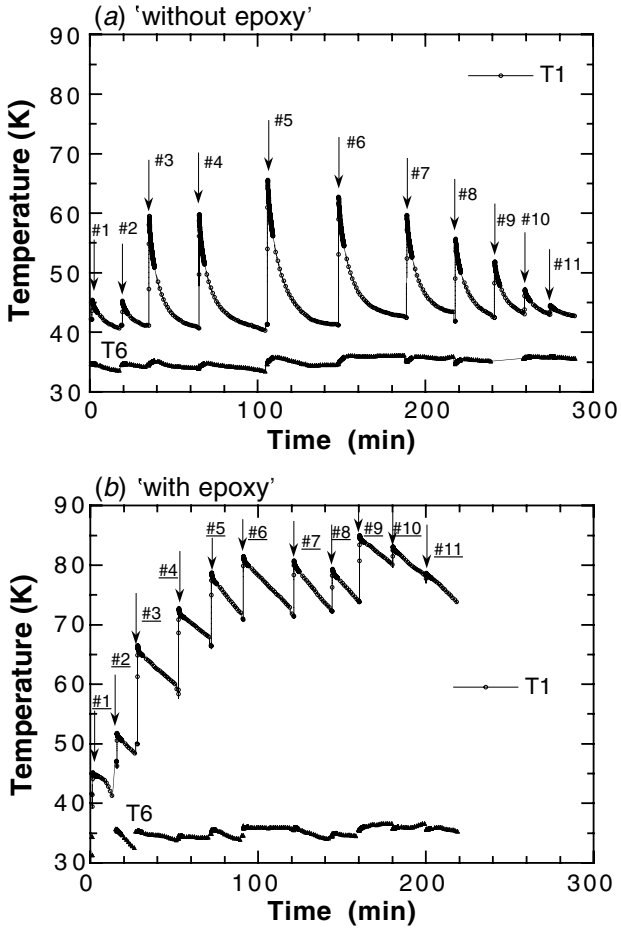

Figure 2. The full time dependences of the typical temperatures ($T\,1$, and $T\,6$) in the IMRA method for the (a) 'without epoxy' setting and (b) 'with epoxy' setting.

Figures 2(a) and (b) present the full time dependences of the temperatures $T\,1$ and $T\,6$ after PFMs for 'without epoxy' and 'with epoxy' settings, respectively. In figure 2(a), the surface temperature suddenly increases just after applying the magnetic pulse and then smoothly decreases to the initial temperature within ∼30 min. The temperature $T\,6$ of the cold stage is nearly independent of the pulse field strength. The maximum temperature rise $\Delta T\,1_{max}$ increases with increasing pulse field strength. In figure 2(b) for the 'with epoxy' setting, the temperature of the bulk surface cannot recover to the initial temperature within several decade minutes and, as can be seen, just before applying the following pulse the surface temperature gradually increases, in spite of the nearly constant $T\,6$. These results confirm that good heat exhaust cannot be realized due to the existence of the epoxy resin layer between the bulk and the cold stage.

Figure 3(a) shows the relation between the trapped magnetic field $B_T{}^P$ by PFM method and the applied pulse field B_{ex} for both 'without epoxy' and 'with epoxy' settings. For the 'without epoxy' setting, the magnetic flux is hardly trapped for the #1 and #2 pulses at the position of the Hall sensor near the central position, and the #3

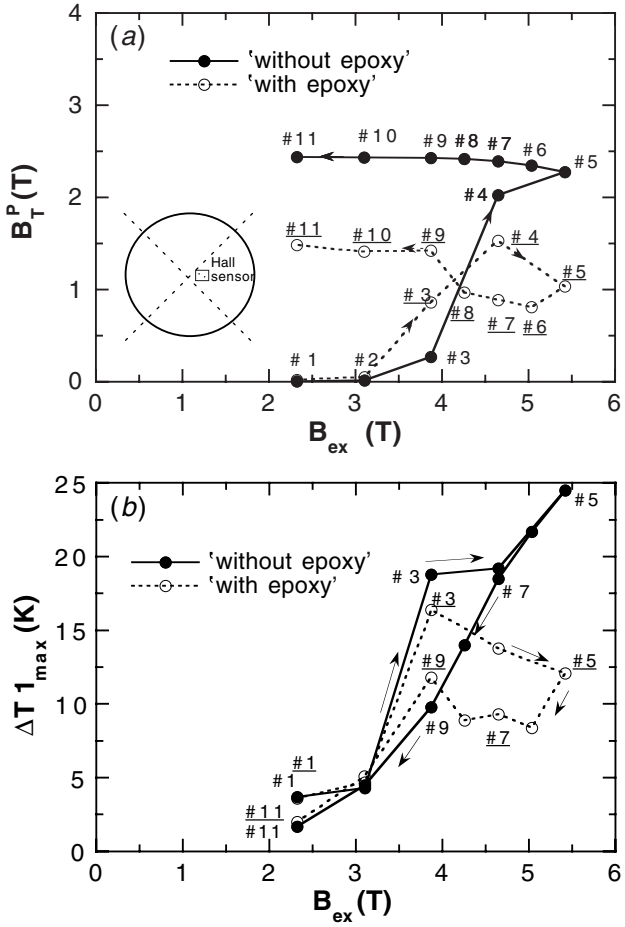

Figure 3. (*a*) The relation between the trapped magnetic field $B_T{}^P$ measured by the attached Hall sensor and the applied pulse field B_{ex}, and (*b*) the relation between the maximum temperature rise $\Delta T\,1_{max}$ of $T\,1$ and B_{ex} for both 'without epoxy' and 'with epoxy' settings.

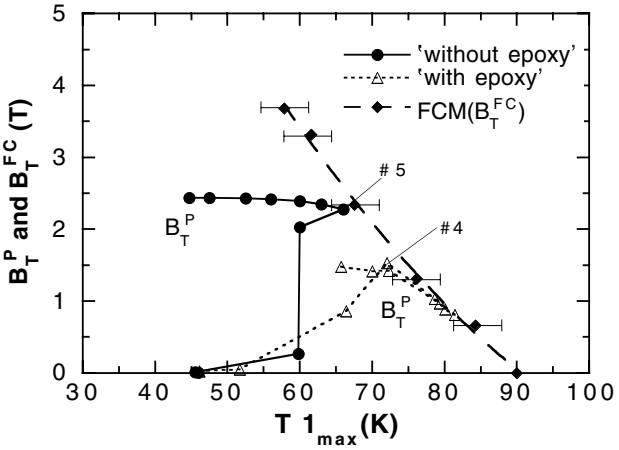

Figure 4. The trapped field $B_T{}^P$ versus the maximum temperature of $T\,1$ ($T\,1_{max}$) after applying the pulse field for 'without epoxy' and 'with epoxy' settings. The trapped field by the FC magnetizing $B_T{}^{FC}$ was also presented.

pulse (B_{ex} = 3.870 T) can give a slight trap ($B_T{}^P$ = 0.271 T). Figure 3(*b*) shows the relation between the maximum temperature rise $\Delta T\,1_{max}$ and B_{ex}. $\Delta T\,1_{max}$ after the #3 pulse is extremely large ($\Delta T\,1_{max}$ = 18.8 K) and the maximum surface temperature $T\,1_{max}$ reaches ∼60 K. Then $B_T{}^P$ suddenly increases to 2.029 T for the #4 pulse (B_{ex} = 4.644 T) and moderately increases to 2.278 T for the #5 (B_{ex} = 5.418 T) pulse. For the following pulses from #6 to #11 with gradually reduced B_{ex} values, $B_T{}^P$ only slightly increases. It was reported that the total trapped flux over the bulk increases through these pulses [2]. $\Delta T\,1_{max}$ versus B_{ex} can be regarded as a smooth relation except for the case of the #3 pulse. For the 'with epoxy' setting, the trapped field $B_T{}^P$ is generally lower and the $B_T{}^P$ versus B_{ex} curve becomes more complicated than for the 'without epoxy' setting. These results may come from the temperature difference of the bulk between both settings before applying each magnetic pulse.

Figure 4 displays the relation between the trapped field $B_T{}^P$ and the maximum temperature $T\,1_{max}$ after applying the pulse field for both settings. The temperature dependence of the trapped field $B_T{}^{FC}$ by the FCM method is also presented in the figure. $B_T{}^{FC}(T)$ decreased with increasing bulk surface temperature $T\,1_{max}$. The maximum temperature rise $\Delta T\,1_{max}{}^{FC}$ was also monitored during the FCM operation, which was as small as ∼4 K [10]. It was found that $B_T{}^P$ could not exceed $B_T{}^{FC}$ for the same bulk surface temperature. In the 'without epoxy' setting, $B_T{}^P$ touches the $B_T{}^{FC}$–$T\,1_{max}$ line for the #5 pulse and then deviates from this line for the succeeding pulses. In the 'with epoxy' setting, $B_T{}^P$ also touches the $B_T{}^{FC}$–$T\,1_{max}$ line ($B_T{}^P$ = 1.5 T at $T\,1_{max}$ = 73 *K*) for the #4 pulse and then decreases along this line for succeeding pulses (#6–#9), because the maximum temperature of the bulk crosses the $B_T{}^{FC}$–$T\,1_{max}$ line. Thus the field trapping ability due to the PFM technique can be systematically explained on the basis of the maximum temperature of the bulk surface. The cold stage temperature $T\,6$ of the GM refrigerator is, at best, the starting temperature of the bulk crystal before the pulse. The temperature monitor of the bulk is indispensable to analyse the PFM technique and to take the full advantage of the IMRA method. The present results are the first experimental confirmation that the decrease of $B_T{}^P$ for higher B_{ex} pulses is attributable to the $B_T{}^{FC}$–$T\,1_{max}$ line limitation and that the $B_T{}^P$ decrease occurs along this line.

3.2. Position dependence of temperature rise

It is widely accepted that the magnetic fluxes penetrate into the bulk crystal preferentially through the weaker pinning regions of the superconductors [4]. The 4-fold GSBs may act as efficient pinning centres for the magnetic fluxes. The position dependence of the temperature rise $\Delta T(t)$ after applying the magnetic pulse should also provide useful information as for the magnetizing mechanism of the PFM technique. Figures 5(*a*) and (*b*) show the time evolution of the normalized temperature rises ($\Delta T_N(t)$(=$\Delta T(t)/\Delta T_{max}$) of $T\,1$–$T\,5$ ($\Delta T\,1_N$–$\Delta T\,5_N$) for the 'without epoxy' setting after applying the #3 and #9 pulses, respectively. The strength of both magnetic pulses is the same (=3.870 T). Since the position dependence of the temperature rise $\Delta T(t)$ is small, the normalized temperature raises $\Delta T_N(t)$ are introduced for clarity. Because the pulse width is as short as a millisecond order, the heat generation should also occur within a millisecond order.

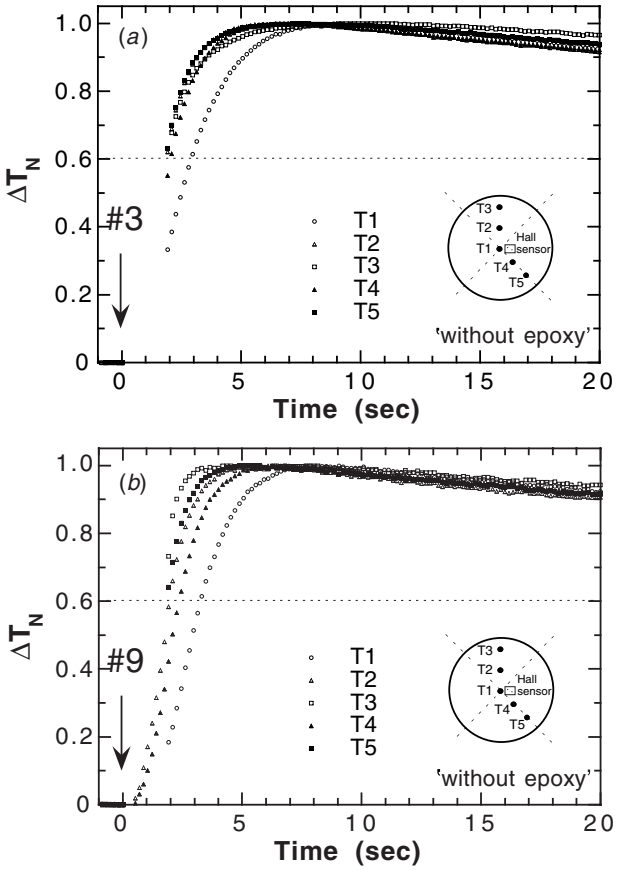

Figure 5. The time dependence of the normalized temperature rises $\Delta T_N(t)$ of $T1$–$T5$ for the 'without epoxy' setting just after applying the (*a*) #3 and (*b*) #9 pulses.

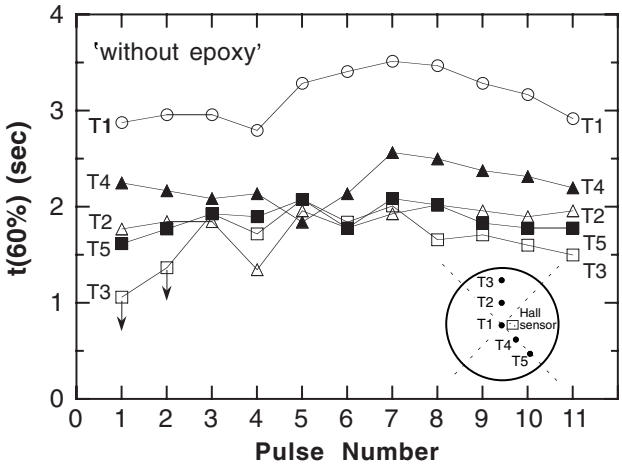

Figure 6. The rising time of $T1$–$T5$ to reach the 60% of the maximum temperature rise $\Delta T_{\max}$ after applying each pulse for 'without epoxy' setting.

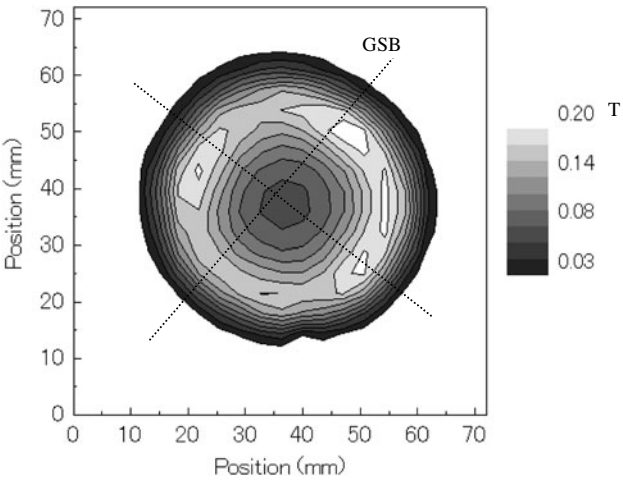

Figure 7. An example of the distribution of the trapped magnetic field above 3 mm on the bulk surface after applying the #1 pulse for 'without epoxy' setting.

For the #3 pulse in figure 5(*a*), $\Delta T1_N(t)$ rises more slowly and the rising times of $\Delta T2_N(t)$–$\Delta T5_N(t)$ are hardly different. On the other hand, for the #9 pulse shown in figure 5(*b*), which resulted in the trapped field of $B_T{}^P = 2.403$ T at the central position, the rising times of $\Delta T2_N$–$\Delta T5_N$ are clearly different; the temperature rise is the fastest for $\Delta T3_N(t)$ and then becomes slower for $\Delta T5_N(t)$, $\Delta T2_N(t)$, $\Delta T4_N(t)$ and $\Delta T1_N(t)$ in this order. Thus the temperature rising time depends on the pulse number or the strength of the pulse field. We define the rising time to reach 60% of the maximum change $\Delta T_{\max}$ after applying the pulse as the rising time $t\,(60\%)$. Figure 6 shows $t\,(60\%)$ of $T1$–$T5$ for each applied pulse. In the case of the #1 and #2 pulses, $T3$ along the bisect line rises first, followed by $T5$ on the GSB line. This result suggests that the applied magnetic flux prefers to penetrate into the bulk through the inter-GSB region of the bulk crystal, avoiding the GSB lines. The more violent flux motion produces more heat in the inter-GSB region, resulting in the faster temperature rise along the bisect line ($T3$, $T2$, $T1$) than that along the GSB line ($T5$, $T4$, $T1$). For the respective series of temperature measurements ($T3$, $T2$, $T1$) and ($T5$, $T4$, $T1$), the temperature rises firstly at the outer positions ($T3$, $T5$), secondly at the inner positions ($T2$, $T4$) and lastly $T1$ rises. The similar behaviours are observable for the #8–#11 pulses. In this way, the heat generation due to the intrusion of the magnetic fluxes occurs faster in the outer positions of the bulk. The slower temperature rise of $T1$ may originate as a result of the heat propagation from outer sides, which is controlled by the thermal diffusivity α_{ab} of the bulk crystals ($\alpha_{ab} \simeq$ 20–10 mm^2 s^{-1} for the temperature range 40–70 K [9]). In the case of #4 to #7 pulses with the $B_{\rm ex}$ strength higher than ∼4 T, $t\,(60\%)$ of both series of ($T3$, $T2$, $T1$) and ($T5$, $T4$, $T1$) is not explicitly arranged in this order. As we have mentioned, the magnetic fluxes arrive at the position of the Hall sensor near the central region for the #4 pulse and the flux motion may become complicated under the following strong magnetic pulses. It is worthwhile noting, however, that the rising time of $T2$ is consistently faster than that of $T4$.

Figure 7 shows an example of the distribution of the trapped magnetic field above 3 mm from the bulk surface after applying the #1 pulse for the 'without epoxy' setting. The sample arrangement of this figure is the same as that in figure 1(*d*). The distribution of trapped magnetic field shows a faint 4-fold symmetry, the magnetic fluxes being trapped along GSBs somewhat more strongly than those in the inter-GSB region. These results also support that there is a larger density

of pinning centres along the GSBs than in the inter-GSB region and are consistent with the analyses of the position dependence of ΔT.

4. Summary

The time evolution and position dependence of the temperature rise Delta $T(t, r)$ on the surface of the cryo-cooled YBaCuO bulk superconductor has been measured after the pulse field magnetizing (PFM). Important experimental results and conclusions obtained in this study are summarized as follows.

(1) The epoxy resin, which is impregnated and coated on the bulk superconductor for the mechanical reinforcement, strongly prevents the heat exhaust from the bulk to the cold stage of the refrigerator. It needs much time for the resin-impregnated superconductor to recover the initial temperature (∼the cold stage temperature) after being heated by the applied pulse field.

(2) The maximum temperature rise $\Delta T_{\max}$ after applying the pulse field increases with increasing magnetic pulse field strength and an anomalously large temperature rise ($\Delta T_{\max} \sim 18.8$ K) is observed just before the magnetic field is trapped in the vicinity of the centre of the bulk.

(3) It has been experimentally confirmed that the trapped field ${B_T}^P$ by PFM cannot exceed the trapped field ${B_T}^{\mathrm{FC}}$ by the static field cooled magnetizing (FCM) at the same bulk temperature. These results could be clarified by measuring the maximum temperature $T_{\max}$ of the bulk surface after the pulse field application.

(4) The time evolution of temperature rise $\Delta T(t)$ depends on the position on the bulk surface and the magnetic fluxes move more easily through the inter-GSB region which is surrounded by the growth sector boundaries (GSBs). The temperature rise first occurs at the outer region of the bulk crystal and then heat propagates to the centre of the bulk crystal. These results are consistent with the distribution of the trapped field.

(5) The *in situ* temperature monitor on the bulk surface gives us valuable information about the magnetizing mechanism of the bulk superconductors and is indispensable to the PFM analyses. The efficiency of the IMRA method must be tested by monitoring the bulk sample temperature to take full advantage of the iterative pulse techniques.

Acknowledgments

This work is partially supported by Japan Science and Technology Corporation under the Joint-research Project for Regional Intensive in the Iwate Prefecture on Development of practical applications of magnetic field technology for use in the region and in everyday living.

References

[1] Itoh Y and Mizutani U 1996 *Japan. J. Appl. Phys.* **35** 2114
[2] Mizutani U, Oka T, Itoh Y, Yanagi Y, Yoshikawa M and Ikuta H 1998 *Appl. Supercond.* **6** 235
[3] Ikuta H, Yanagi Y, Yoshikawa M, Itoh Y, Oka T and Mizutani U 2001 *Physica* C **357–360** 837
[4] Ishihara H, Ikuta H, Itoh Y, Yanagi Y, Yoshikawa M, Oka T and Mizutani U 2001 *Physica* C **357–360** 763
[5] Oka T, Yokoyama K, Itoh Yanagi Y, Yoshikawa M, Ikuta H, Mizutani U, Okada H and Noto K 2003 *Physica* C at press
[6] Ikuta H, Ishihara H, Hosokawa T, Yanagi Y, Itoh Y, Yoshikawa M, Oka T and Mizutani U 2000 *Supercond. Sci. Technol.* **13** 846
[7] Tomita M and Murakami M 1999 *J. Cryo. Soc. Jpn.* **34** 616
[8] Sample H H, Neuringer L J and Rubin L G 1974 *Rev. Sci. Instrum.* **45** 64
[9] Fujishiro H, Ikebe M, Naito T, Noto K, Kohayashi S and Yoshizawa S 1994 *Japan. J. Appl. Phys.* **33** 4965
[10] Oka T, Fujishiro H, Yokoyama K and Noto K 2003 unpublished